1

Basic mechanics of rotor systems and helicopter flight

1.1 Introduction

In this chapter we shall discuss some of the fundamental mechanisms of rotor systems from both the mechanical system and the kinematic motion and dynamics points of view. A brief description of the rotor hinge system leads on to a study of the blade motion and rotor forces and moments. Only the simplest aerodynamic assumptions are made in order to obtain an elementary appreciation of the rotor characteristics. It is fortunate that, in spite of the considerable flexibility of rotor blades, much of helicopter theory can be effected by regarding the blade as rigid, with obvious simplifications in the analysis. Analyses that involve more detail in both aerodynamics and blade properties are made in later chapters. The simple rotor system analysis in this chapter allows finally the whole helicopter trimmed flight equilibrium equations to be derived.

1.2 The rotor hinge system

The development of the autogyro and, later, the helicopter owes much to the introduction of hinges about which the blades are free to move. The use of hinges was first suggested by Renard in 1904 as a means of relieving the large bending stresses at the blade root and of eliminating the rolling moment which arises in forward flight, but the first successful practical application was due to Cierva in the early 1920s. The most important of these hinges is the *flapping* hinge which allows the blade to flap, i.e. to move in a plane containing the blade and the shaft. Now a blade which is free to flap experiences large Coriolis moments in the plane of rotation and a further hinge – called the *drag* or *lag* hinge – is provided to relieve these moments. Lastly, the blade can be *feathered* about a third axis, usually parallel to the blade span, to enable the blade pitch angle to be changed. A diagrammatic view of a typical hinge arrangement is shown in Fig. 1.1.

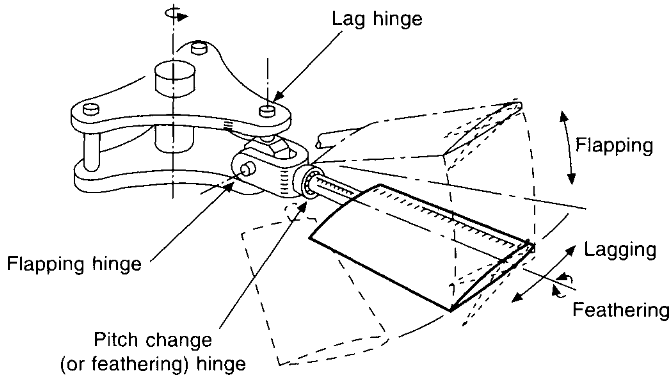

Fig. 1.1 Typical hinge arrangement

In this figure, the flapping and lag hinges intersect, i.e. the hinges are at the same distance from the rotor shaft, but this need not necessarily be the case in a particular design. Neither are the hinges always absolutely mutually perpendicular.

Consider the arrangement shown in Fig. 1.2. Let OX be taken parallel to the blade-span axis and OZ perpendicular to the plane of the rotor hub. Let OP represent either the flapping hinge axis or the lag hinge axis. The flapping hinge is referred to as the δ-hinge and the lag hinge as the α-hinge. We then define:

- the angle between OZ and the projection of OP onto the plane OYZ as δ_1 or α_1,
- the angle between OZ and the projection of OP onto the plane OXZ as δ_2 or α_2,
- the angle between OY and the projection of OP onto the plane OXY as δ_3 or α_3.

These are the definitions in common use in industry. The most important angles in practice are α_2, which leads to pitch resulting from lagging of the blade, and δ_3, which couples pitch and flap, as follows.

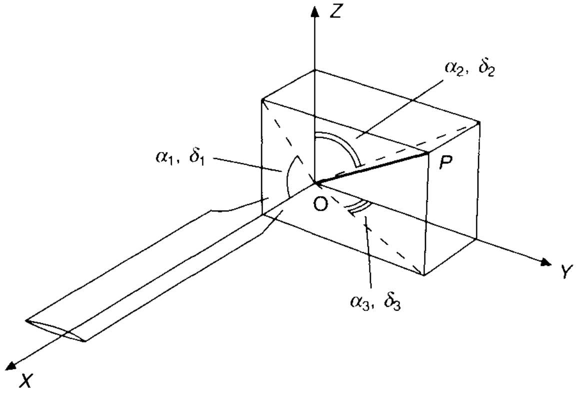

Fig. 1.2 Blade hinge angles

Referring to Fig. 1.3, when δ_3 is positive, positive blade flapping causes the blade pitch angle to be reduced. It will also be appreciated that, if the drag hinge is mounted outboard of the flapping hinge, movement about the lag hinge produces a δ_3 effect. If the blade moves through angle ξ_0 and flaps through angle β relative to the hub plane, the change of pitch angle $\Delta\theta$ due to flapping is found to be

$$\Delta\theta = -\tan\beta \tan(\delta_3 - \xi_0)$$

or for small angles

$$\Delta\theta = -\beta \tan(\delta_3 - \xi_0)$$

so $\Delta\theta$ is proportional to β.

The dynamic coupling of blade motions will be dealt with in more detail in Chapter 9.

The blades of two-bladed rotors are usually mounted as a single unit on a 'see-saw' or 'teetering' hinge, Fig. 1.4(a). No lag hinges are fitted, but the Coriolis root

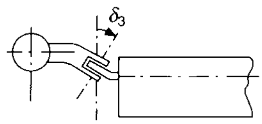

Fig. 1.3 The δ_3-hinge

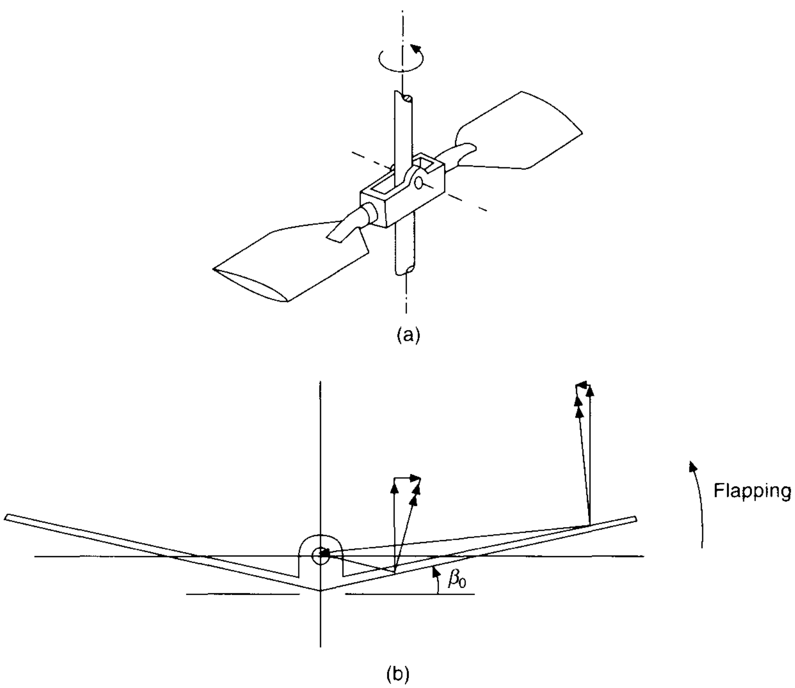

Fig. 1.4 (a) Teetering or see-saw rotor. (b) Underslung rotor, showing radial components of velocity on upwards flapping blade

bending moments may be greatly reduced by 'underslinging' the rotor Fig. 1.4(b). It can be seen from the figure that, when the rotor flaps, the radial components of velocity of points on the upwards flapping blade below the hinge line are positive while those above are negative. Thus the corresponding Coriolis forces are of opposite sign and, by proper choice of the hinge height, the moment at the blade root can be reduced to second order magnitude. This assumes that a certain amount of pre-cone or blade flap, β_0, is initially built in.

Although, as stated earlier, the adoption of blade hinges was an important step in the evolution of the helicopter, several problems are posed by the presence of hinges and the dampers which are also fitted to restrain the lagging motion. Not only do the bearings operate under very high centrifugal loads, requiring frequent servicing and maintenance, but when the number of blades is large the hub becomes very bulky and may contribute a large proportion of the total drag. Figure 1.5(a) shows a diagrammatic view of the Westland Wessex hub, on which, as may be observed, the flapping and lag hinges intersect. Figure 1.5(b) is a photograph of the same rotor hub, showing also the swash plate mechanism that enables the cyclic and collective pitch control (discussed in section 1.7).

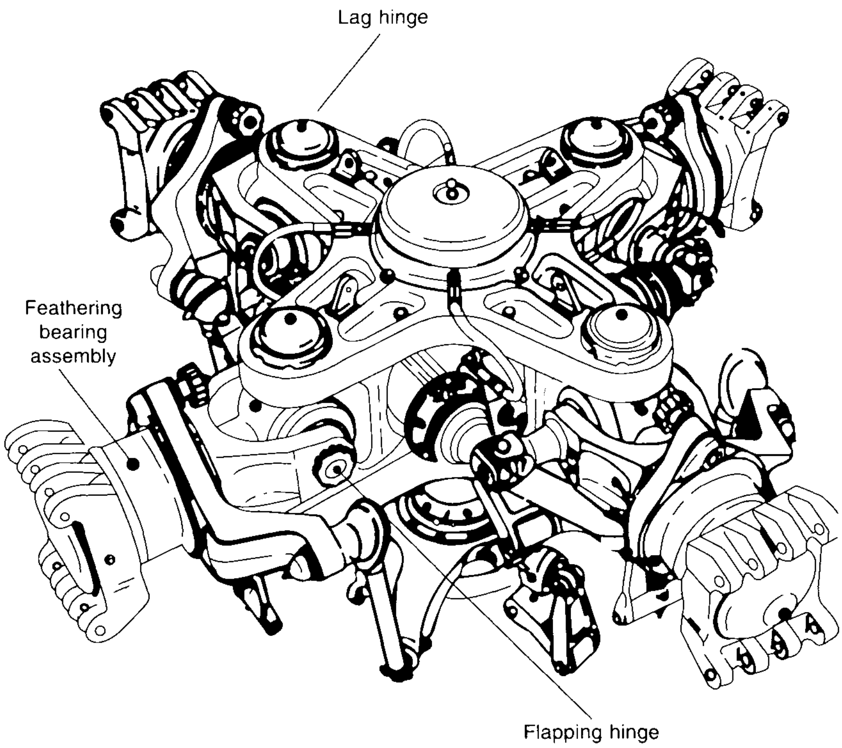

Fig. 1.5 (a) Diagrammatic view of Westland Wessex hub

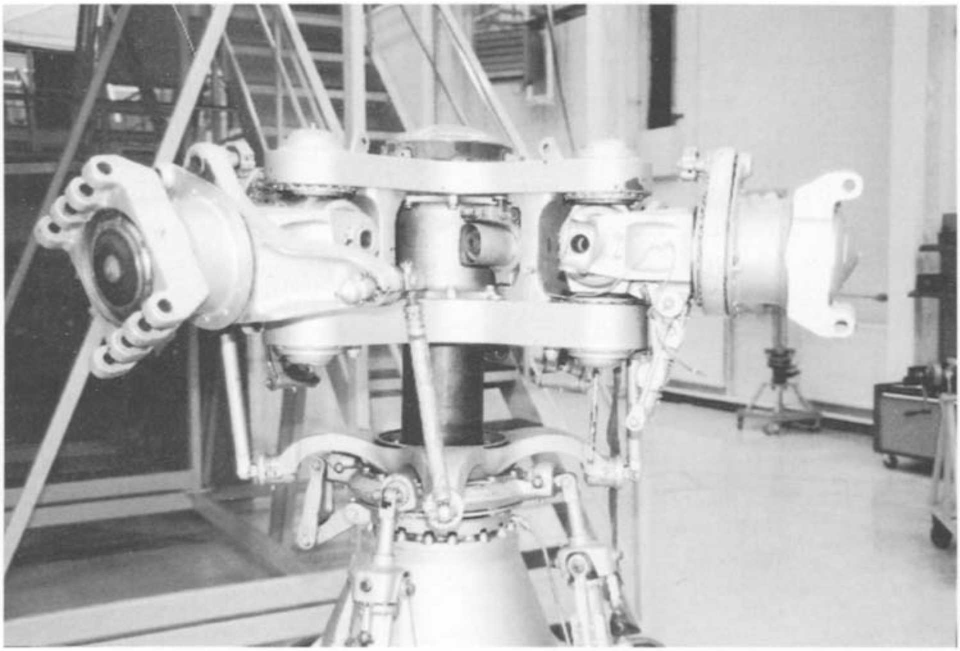

Fig. 1.5 (b) Photograph of Westland Wessex hub

More recently, improvements in blade design and construction enabled rotors to be developed which dispensed with the flapping and lagging hinges. These 'hingeless', or less accurately termed 'semi-rigid', rotors have blades which are connected to the shaft in cantilever fashion but which have flexible elements near to the root, allowing the flapping and lagging freedoms. Such a design is shown in Fig. 1.6(a) which is that of the Wesland Lynx helicopter. In this case, the flexible element is close in to the rotor shaft, with the feathering hinge between it and the flexible lag element, which is the furthest outboard. The diagram also indicates the attached lag dampers mentioned previously, and discussed in relation to ground resonance in Chapter 9, and a different, but less common, mechanism for changing the cyclic and collective pitch on the blades. A photograph of the same hub design, but with five blades, is shown in Fig. 1.6(b). Rotor hub designs for current medium to large helicopters commonly use a high proportion of composite material for the main structural elements, with elastomeric elements providing freedoms where only low stiffnesses are required (e.g. to allow blade feathering).

We now derive the equations of flapping, lagging, and feathering motion of the hinged blade – but assuming it to be rigid, as mentioned in the introduction. The motion of the hingeless blade will be considered in Chapter 7. Fortunately, except for the lagging motion, the equations can be derived with sufficient accuracy by treating each degree of freedom separately, e.g. in considering flapping motion it can be assumed that lagging and feathering do not occur.

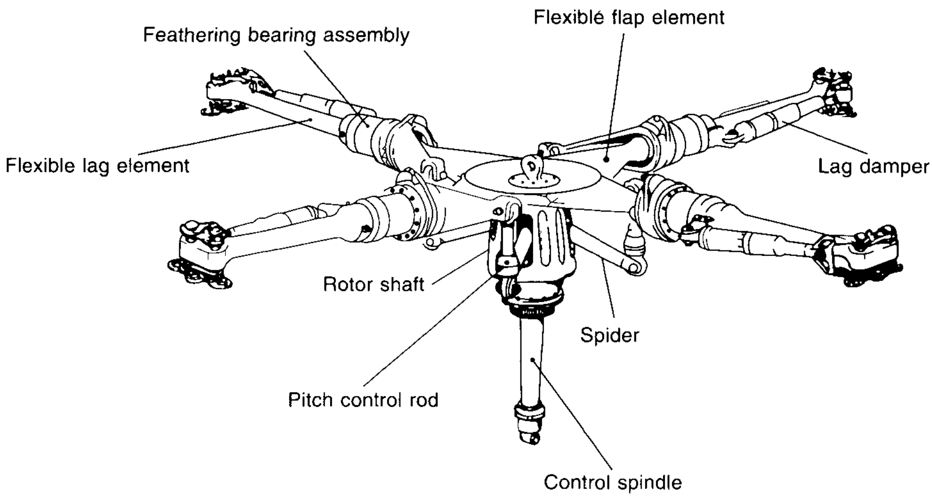

Fig. 1.6 (a) Diagrammatic view of Westland Lynx hub

Fig. 1.6 (b) Photograph of Westland Lynx five-bladed hub

1.3 The flapping equation

Consider a single blade as shown in Fig. 1.7 and let the flapping hinge be mounted a distance eR from the axis of rotation. The shaft rotates with constant angular velocity Ω and the blade flaps with angular velocity $\dot{\beta}$. Take axes fixed in the blade, parallel to the principal axes, origin at the hinge, with the $\boldsymbol{i}$ axis along the blade span, the $\boldsymbol{j}$ axis perpendicular to the span and parallel to the plane of rotation, and the $\boldsymbol{k}$ axis completing the right-hand set. To a very good approximation the blade can be treated as a lamina.

Then, if A is the moment of inertia about $\boldsymbol{i}$, and B the moment of inertia about $\boldsymbol{j}$, the moment of inertia C about $\boldsymbol{k}$ is equal to $A + B$. The angular velocity components ω_1, ω_2, ω_3 about these axes are

$$\omega_1 = \Omega \sin \beta, \quad \omega_2 = -\dot{\beta}, \quad \omega_3 = \Omega \cos \beta$$

The acceleration, $\boldsymbol{a}_0$, of the origin is clearly $\Omega^2 eR$ and perpendicular to the shaft. Along the principal axes the components are

$$\{-\Omega^2 \, eR \cos \beta, \quad 0, \quad \Omega^2 \, eR \sin \beta\}$$

The position vector of the blade c.g. is $\boldsymbol{r}_g = x_g R\boldsymbol{i}$, so that the components of $\boldsymbol{r}_g \times \boldsymbol{a}_0$ are

$$\{0, \, ex_g \, \Omega^2 R^2 \sin \beta, \, 0\}$$

The flapping motion takes place about the $\boldsymbol{j}$ axis, so putting the above values in the second of the 'extended' Euler's equations derived in the appendix (eqn A.1.15), and using $A + B = C$, gives

$$B\ddot{\beta} + \Omega^2(B \cos \beta + M_b e x_g R^2) \sin \beta = M_A \tag{1.1}$$

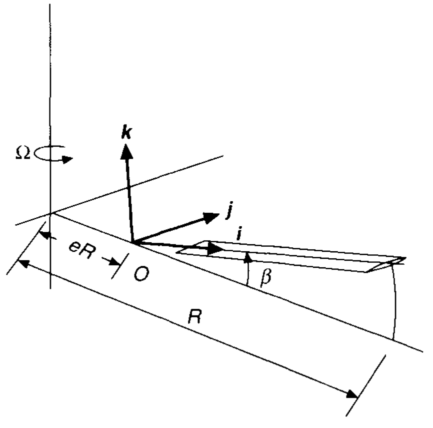

Fig. 1.7 Single flapping blade

where $M_A = -M$ is the aerodynamic moment in the sense of positive flapping and M_b is the blade mass. For small flapping angles eqn 1.1 can be written

$$\ddot{\beta} + \Omega^2(1 + \varepsilon)\,\beta = M_A/B \tag{1.2}$$

where $\varepsilon = M_b e x_g R^2/B$.

If the blade has uniform mass distribution, it can easily be verified that $\varepsilon = 3e/2\ (1 - e)$. A typical value of e is 0.04, giving ε as approximately 0.06.

The flapping equation (eqn 1.1) could also have been derived by considering an element of the blade of mass dm, and at a distance r from the hinge, to be under the action of a centrifugal force $(eR + r\cos\beta)\,\Omega^2\,\mathrm{d}m$ directed outwards and perpendicular to the shaft. The integral of the moment of all such forces along the blade is found to be the second term of eqn 1.1, i.e. $\Omega^2(B\cos\beta + M_b e x_g R^2)\sin\beta$. Regarding it as an external moment like M_A, this centrifugal moment (for small β) acts like a torsional spring tending to return the blade to the plane of rotation.

The other two extended Euler's equations (eqns A.1.17 and A.1.19) give

$$L = 0 \text{ and } N = -2B\Omega\dot{\beta}\sin\beta$$

These are the moments about the feathering and lag axes, respectively, which are required to constrain the blade to the flapping plane, or, in other words, $-L$ and $-N$ are the couples which the blade exerts on the hub due to flapping only. It can be seen that flapping produces no feathering inertia moment, but the in-plane moment $2B\Omega\dot{\beta}\sin\beta$ is often so large that it is usually relieved by the provision of a lag hinge or equivalent flexibility, as mentioned in section 1.2. This moment is the moment of the Coriolis inertia forces acting in the in-plane direction.

More generally, if the rotor hub is pitching with angular velocity q, Fig. 1.8, the angular velocity components of the blade are

$$\{q\sin\psi\cos\beta + \Omega\sin\beta,\quad q\cos\psi - \dot{\beta},\quad -q\sin\psi\sin\beta + \Omega\cos\beta\}$$

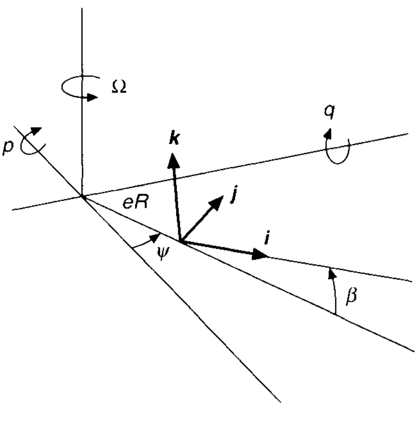

Fig. 1.8 Blade influenced by rotor hub pitching velocity q and rolling velocity p

where ψ is the *azimuth* angle of the blade, defined as the angle between the blade span and the rear centre line of the helicopter. The absolute accelerations of the hinge point O are the centripetal acceleration $\Omega^2 eR$ acting radially inwards and $eR(\dot{q}\cos\psi - 2q\Omega\sin\psi)$ acting normal to the plane of the rotor hub.

Inserting these values into eqn A.1.15 and neglecting q^2, which is usually very small compared with Ω^2, we finally obtain after some manipulation

$$\ddot{\beta} + \Omega^2(1+\varepsilon)\beta = M_A/B - 2\Omega q(1+\varepsilon)\sin\psi + \dot{q}(1+\varepsilon)\cos\psi \qquad (1.3)$$

The second term on the right is the gyroscopic inertia moment due to pitching velocity, and the third term is due to the pitching acceleration.

We now find that the feathering moment L is

$$L = A(2\Omega q\cos\psi + \dot{q}\sin\psi)$$

which means that the pitching motion produces a moment tending to twist the blade. The moment about the lag axis is hardly affected by the pitching motion, so that N remains as before.

When the rotor hub is rolling with angular velocity p, Fig. 1.8, the equivalent equation to 1.3 may be derived in like manner, and in this case the extra terms on the right-hand side can be shown to be $(1+\varepsilon)(2\Omega p\cos\psi + \dot{p}\sin\psi)$.

1.4 The equation of lagging motion

We assume the flapping angle to be zero and that the blade moves forward on the lag hinge through angle ξ (Fig. 1.9). The angular velocity of the blade is $(\Omega + \dot{\xi})\boldsymbol{k}$ and $\boldsymbol{a}_0 = -\Omega^2 eR(\cos\xi\boldsymbol{i} - \sin\xi\boldsymbol{j})$. Then the third of Euler's extended equations gives

$$C\ddot{\xi} + Mex_g\Omega^2R^2\sin\xi = N \qquad (1.4)$$

or, for small ξ,

$$\ddot{\xi} + \Omega^2\varepsilon\xi = N/C \qquad (1.5)$$

where ε, in this case, is $M_b ex_g R^2/C$, eR being the drag-hinge offset distance.

It can easily be verified that if flapping motion is also included, the only important term arising is the moment $2B\Omega\beta\dot{\beta}$ calculated in the previous section. With a lag

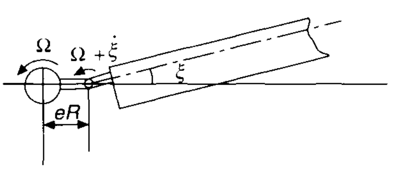

Fig. 1.9 Blade lagging

hinge fitted, this moment can be regarded as an inertia moment and considered as part of N. Then, if N_A is taken as the aerodynamic lagging moment, together with any artificial damping which may be, and usually is, added, eqn 1.5 can be written finally as

$$\ddot{\xi} + \Omega^2\varepsilon\xi - 2\Omega\beta\dot{\beta} = N_A/C \text{ (since } B \approx C) \tag{1.6}$$

The lagging motion produces no moment about the feathering axis, but the instantaneous angular velocity $\Omega + \dot{\xi}$ will affect the centrifugal and aerodynamic flapping moments and may have to be taken into account when considering coupled motion (see section 9.7).

1.5 Feathering motion

It is assumed that the flapping and lagging angles are zero and that the blade feathers through angle θ (Fig. 1.10). The angular velocity components about $\boldsymbol{i}$, $\boldsymbol{j}$, $\boldsymbol{k}$ are $\dot{\theta}$, $\Omega \sin \theta$, $\Omega \cos \theta$. The first of Euler's extended equations gives

$$A\dot{\theta} + A\Omega^2 \sin \theta \cos \theta = L \tag{1.7}$$

and, for the small feathering angles which normally occur, we can write

$$\ddot{\theta} + \Omega^2\theta = L/A \tag{1.8}$$

The second and third of Euler's equations show that the feathering motion produces no flapping moment but a lagging moment of $-2A\dot{\theta}\Omega \sin \theta$. This latter moment is extremely small compared with the flapping Coriolis moment and can be neglected.

1.6 Flapping motion in hovering flight

The equation of blade flapping (1.2) is

$$d^2\beta/dt^2 + \Omega^2(1 + \varepsilon)\beta = M_A/B$$

It is convenient to change the independent variable from time to blade azimuth angle by means of $\psi = \Omega t$. Then since

$$d/dt = \Omega d/d\psi \quad \text{and} \quad d^2/dt^2 = \Omega^2 d^2/d\psi^2$$

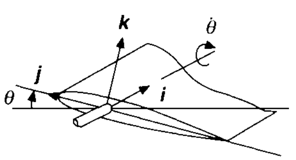

Fig. 1.10 Blade feathering

eqn 1.2 becomes

$$d^2\beta/d\psi^2 + (1 + \varepsilon)\beta = M_A/B\Omega^2 \quad (1.9)$$

This equation is valid for any case of steady rectilinear flight including hovering. The problem is to express M_A as a function of ψ and then to solve the equation. We now consider some simple but important examples in hovering flight.

1.6.1 Disturbed flapping motion at constant blade pitch angle

We suppose that the blades are set at a constant blade pitch angle relative to the shaft and that the rotor is rotating steadily with angular velocity Ω. Since we are interested only in the character of the disturbed motion, the aerodynamic moment corresponding to the constant pitch angle will be ignored and attention will be concentrated on the aerodynamic moments arising from disturbed flapping motion.

Now, when a blade flaps with angular velocity $\dot{\beta}$, there is a relative downwash of velocity $r\dot{\beta}$ at a point on the blade distance r from the hinge. Assuming $\cos\beta = 1$, the chordwise component of wind velocity is $\Omega(r + eR)$, so that the local change of incidence $\Delta\alpha$ due to flapping is

$$\Delta\alpha = \frac{-r\dot{\beta}}{(r + eR)\Omega} = \frac{-x\, d\beta/d\psi}{x + e}$$

where $x = r/R$.

Assuming a constant lift slope a for the blade section, the lift on an element of blade is

$$dL = -\tfrac{1}{2}\rho ac\Omega^2 R^3(x + e)x(d\beta/d\psi)\,dx$$

The moment of this lift about the flapping hinge is $r\,dL$ and the total aerodynamic moment, assuming the blade chord c to be constant, is

$$M_A = \int_0^{R(1-e)} r\,dL = -\tfrac{1}{2}\rho ac\Omega^2 R^4 \int_0^{(1-e)} x^2(x + e)(d\beta/d\psi)dx$$

giving

$$M_A/B\Omega^2 = -(\gamma/8)(1 - e)^3(1 + e/3)d\beta/d\psi$$

where $\gamma = \rho acR^4/B$ is called *Lock's inertia number.*

Writing n for $(1 - e)^3(1 + e/3)$, the flapping equation becomes

$$d^2\beta/d\psi^2 + (n\gamma/8)d\beta/d\psi + (1 + \varepsilon)\beta = 0 \quad (1.10)$$

Equation 1.10 is the equation of damped harmonic motion with a natural undamped frequency $\Omega\sqrt{(1 + \varepsilon)}$. If ε is zero (no flapping hinge offset), the natural undamped frequency is exactly equal to the shaft frequency. Normally ε is about 0.06, giving an undamped flapping frequency about 3 per cent higher than the shaft frequency.

Taking a typical value of γ of 6 gives a value for $n\gamma/8$ of about 0.7. This means that the damping of the motion is about 35 per cent of critical, or that the *time-constant* in terms of the azimuth angle is about 90° or $\frac{1}{4}$ of a revolution. Thus, the flapping motion is very heavily damped. It has already been remarked that the centrifugal moment acts like a spring, and we now see that flapping produces an aerodynamic moment proportional to flapping rate, i.e. in hovering flight the blade behaves like a mass–spring–dashpot system. In forward flight the damping is more complicated and includes a periodic component, but the notion of the blade as a second order system is often a useful one in a physical interpretation of blade motion.

1.6.2 Flapping motion due to cyclic feathering

Suppose that, in addition to a constant (collective) pitch angle θ_0, the blade pitch is veried in a sinusoidal manner relative to the hub plane. The blade pitch θ can then be expressed as

$$\theta = \theta_0 - A_1 \cos \psi - B_1 \sin \psi \tag{1.11}$$

To simplify the calculations we will take $e = 0$, since the small values of flapping hinge offset normally employed have little effect on the flapping motion.

In calculating the flapping moment M_A, the induced velocity, or rotor downwash, to be discussed in Chapter 2, will be ignored. By a similar analysis to that above, the flapping moment is easily found to be given by

$$M_A/B\Omega^2 = \gamma(\theta_0 - A_1 \cos \psi - B_1 \sin \psi)/8$$

Substituting in eqn 1.9 leads to the steady-state solution

$$\beta = \gamma\theta_0/8 - A_1 \sin \psi + B_1 \cos \psi \tag{1.12}$$

The term $\gamma\theta_0/8$ represents a constant flapping angle and corresponds to a motion in which the blade traces out a shallow cone, and for this reason the angle is called the *coning angle*. If the induced velocity had been included, the coning angle would have been reduced somewhat. For our present purpose the exact calculation of the coning angle is unimportant. The terms $-A_1 \sin \psi + B_1 \cos \psi$ represent a tilt of the axis of the cone away from the shaft axis. Since ψ is usually measured from the rearmost position of the blade, i.e. along the axis of the rear fuselage, a positive value of B_1 denotes a forward (nose down) tilt of the cone, Fig. 1.11, while a positive value of A_1 denotes a sideways component of tilt in the direction of $\psi = 90°$. The blade tips trace out the 'base' of the cone, which is often referred to as the *tip path plane* or as the *rotor disc*, Fig. 1.11.

In steady flight the blade motion must be periodic and is therefore capable of being expressed in a Fourier series as

$$\beta = a_0 - a_1 \cos \psi - b_1 \sin \psi - a_2 \cos 2\psi - b_2 \sin 2\psi - \dots \tag{1.13}$$

For the case in question,

$$a_0 = \gamma\theta_0/8, \quad a_1 = -B_1, \quad b_1 = A_1$$

$$a_2 = b_2 = \dots \text{ etc.} = 0$$

When the flight condition is steady, eqn 1.9 can always be solved by assuming the

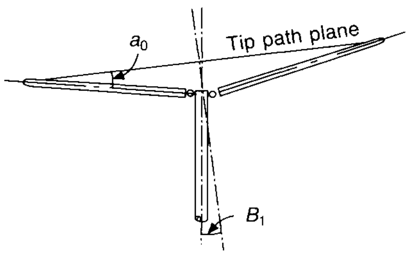

Fig. 1.11 Interpretation of flapping and feathering coefficients

form of eqn 1.13, substituting in the flapping equation, and equating coefficients of the trigonometric terms. This is a method we shall be forced to adopt when the flapping equation contains periodic coefficients, as will be the case in forward flight.

In terms of eqn 1.13, a_0 represents the coning angle and a_1 and b_1 represent respectively, a backward and sideways tilt of the rotor disc, the sideways tilt being in the direction of $\psi = 90°$. The higher harmonics a_2, b_2, a_3,..., etc., which will have non-zero values in forward flight, can be interpreted as distortions or a 'crinkling' of the rotor cone. But although these harmonics can be calculated, the blade displacements they represent are only of the same order as those of the elastic deflections which, so far, have been neglected. Thus, it is inconsistent to calculate the higher harmonics of the rigid blade mode of motion without including the other deflections of the blade. Stewart[1] has shown that the higher harmonics are usually about one tenth of the values of those of the next order above.

Comparison of eqns 1.11 and 1.12 shows that the amplitude of the periodic flapping is precisely the same as the applied cyclic feathering and that the flapping lags the cyclic pitch by 90°. The phase angle is exactly what we might have expected, since the aerodynamic flapping moment forces the blade at its undamped natural frequency and, as is well known, the phase angle of a second order dynamic system at resonance is 90° whatever the damping. Further, the fact that the amplitude of flapping is exactly the same as the applied feathering has a simple physical explanation. Suppose that initially no collective or cyclic pitch were applied; the blades would then trace out a plane perpendicular to the rotor shaft. If cyclic pitch were then applied, and the blades remained in the initial plane of rotation, they would experience a cyclic variation of incidence and, hence, of aerodynamic moment. The moment would cause the blades to flap and, since, as we have found, blade flapping motion is stable, the blades must seek a new plane of rotation such that the flapping moment vanishes. This is clearly a plane in which there is no cyclic feathering and it follows from Fig. 1.12 that this plane makes the same angle to the shaft as the amplitude of the cyclic pitch variation. It is also obvious that the effect of applying cyclic pitch is precisely the same as if cyclic pitch had been absent but the shaft had been tilted through the same angle. Tilting the rotor shaft or, more precisely, the rotor hub plane, is the predominant method of controlling the rotor of an autogyro. Tilting the shaft of a helicopter is impossible if it is driven by a fuselage mounted engine, and the rotor must be controlled by cyclic feathering.

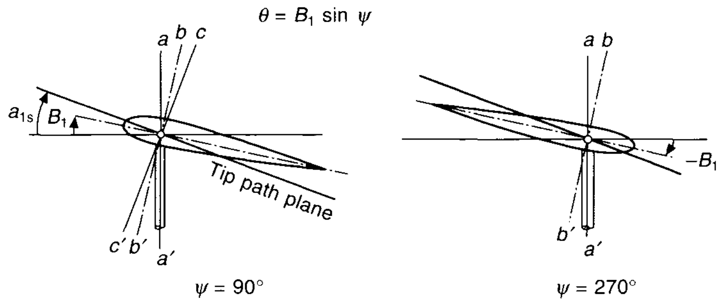

Fig. 1.12 Equivalence of flapping and feathering

The above discussion illustrates the phenomenon of the so-called 'equivalence of feathering and flapping'; the interpretation is a purely geometric one. If flapping and feathering are purely sinusoidal, the amplitude of either depends entirely upon the axis to which it is referred. In Fig. 1.12, *aa′* is the shaft axis, *bb′* is the axis perpendicular to the blade chord, *cc′* the axis perpendicular to the tip path plane. If Fig. 1.12 shows the blade at its greatest pitch angle, *bb′* is clearly the axis relative to which the cyclic feathering vanishes and is called the *no-feathering axis*. Similarly *cc′* is the axis of no flapping.

Let a_{1s} be the angle between the shaft and the tip path plane and B_1 the angle between the shaft and the no-feathering axis. Viewed from the no-feathering axis the cyclic feathering is, by definition, zero but the angle of the tip path plane is $a_{1s} - B_1$. On the other hand, viewed from the tip path plane, the flapping is zero but the feathering amplitude is $B_1 - a_{1s}$. Thus feathering and flapping can be interchanged and either may be made to vanish by the appropriate choice of axis. The ability to select an axis relative to which either the feathering or flapping vanishes is useful in simplifying the analysis of rotor blade motion and for interpreting rotor behaviour. The coning angle a_0 and collective pitch θ_0 play no part in the principle of equivalence.

Strictly speaking, the principle of equivalence fails if the flapping hinges are offset, because the angle of the tip path plane will then no longer be the same as the amplitude of blade flapping, as a sketch will easily show. However, the size of the offset is usually so small that the equivalence idea can be generally applied. Offset hinges, as will be seen later, make an important contribution to the moments on the helicopter.

Another important feature of blade flapping motion can be deduced from the flapping equation. Assuming ε to be negligible, the flapping equation (eqn 1.9) can be written

$$\mathrm{d}^2\beta/\mathrm{d}\psi^2 + \beta = M_A/B\Omega^2$$

in which β is defined relative to a plane perpendicular to the shaft axis.

Now, assuming that higher harmonics can be neglected, steady blade flapping can be expressed in the form

$$\beta = a_0 - a_1 \cos \psi - b_1 \sin \psi$$

and on substitution for β into the flapping equation above

$$M_A = B\Omega^2 a_0 = \text{constant}$$

Thus, for first harmonic motion, the blade flaps in such a way as to maintain a constant aerodynamic flapping moment. This does not necessarily mean that the blade thrust is also constant, since, except in hovering flight, the blade loading distribution varies with azimuth angle and the centre of pressure of the loading moves along the blade.

1.6.3 Flapping motion due to pitching or rolling

An important hovering flight case for which the response of the rotor can be calculated is pitching or rolling. Consider first the case of pitching at constant angular velocity q. The equation of motion, eqn 1.3, with $\varepsilon = 0$, is

$$\mathrm{d}^2\beta/\mathrm{d}t^2 + \Omega^2\beta = M_A/B - 2\Omega q \sin\psi \tag{1.14}$$

Due to pitching and flapping, the velocity component normal to the blade at a point distance r from the hub is $r(q\cos\psi - \dot{\beta})$; with $\cos\beta = 1$ and neglecting a very small term in q, the chordwise velocity is Ωr. The corresponding change of incidence $\Delta\alpha$ is therefore

$$\Delta\alpha = (q\cos\psi - \dot{\beta})/\Omega = \hat{q}\cos\psi - \mathrm{d}\beta/\mathrm{d}\psi$$

where $\hat{q} = q/\Omega$.

The contribution to the flapping moment of the flapping velocity $\dot{\beta}$ has already been considered in section 1.6.1; by a similar calculation the moment due to the pitching velocity q is found to be

$$(M_A)_{\text{pitching}} = \rho ac\Omega^2 R^4 \hat{q}\cos\psi/8 \tag{1.15}$$

Equation 1.14 now becomes

$$\frac{\mathrm{d}^2\beta}{\mathrm{d}\psi^2} + \frac{\gamma}{8}\frac{\mathrm{d}\beta}{\mathrm{d}\psi} + \beta = \frac{\gamma}{8}\hat{q}\cos\psi - 2\hat{q}\sin\psi \tag{1.16}$$

Assuming a steady-state solution, $\beta = a_0 - a_1\cos\psi - b_1\sin\psi$ gives

$$a_1 = -16\hat{q}/\gamma, \qquad b_1 = -\hat{q} \tag{1.17}$$

Hence, when the shaft has a steady positive rate of pitch, the rotor disc tilts forward by amount $16\hat{q}/\gamma$ and sideways (towards $\psi = 270°$) by amount $\hat{q}$. The longitudinal a_1 tilt is due to the gyroscopic moment on the blade, and the lateral b_1 tilt to the aerodynamic moment due to flapping. For typical values of γ, the lateral tilt is roughly half the longitudinal tilt.

The same result can be obtained in a somewhat different way by focusing attention on the rotor disc. If steady blade motion is assumed to occur, each blade behaves identically and the rotor can be regarded as a rigid body rotating in space with angular velocity components Ω about the shaft and q perpendicular to the shaft.

According to elementary gyroscopic theory, the rotor will experience a precessing moment $bC\Omega q$ tending to tilt it laterally towards $\psi = 90°$, bC being the moment of inertia of all the blades in the plane of rotation. In addition, there is the aerodynamic moment on the rotor due to its pitching rotation. Using eqn 1.15, we find that the total moment for *all* the blades is $bC\rho a\Omega^2 R^4 \hat{q}/16$ and is in the nose down sense. Now, these two moments must be in equilibrium with an aerodynamic moment produced by a cyclic pitch variation in the tip path plane, and the rotor achieves this by appropriate tilts a_1 and b_1 relative to the shaft. This cyclic pitch variation, by the arguments of section 1.6.1, is easily seen to be $-a_1 \sin\psi + b_1 \cos\psi$. By comparing this with eqn 1.11, the aerodynamic moment on one blade is seen to be $-B\Omega^2\gamma(a_1 \sin\psi - b_1 \cos\psi)/8$. For *all* blades there would therfore be a steady moment $bB\Omega^2\gamma b_1/16$ acting in the nose down sense and a moment $bB\Omega^2\gamma a_1/16$ in the direction $\psi = 90°$. For these moments to be equal and opposite to those above, we must have, as before,

$$a_1 = -16\hat{q}/\gamma \quad \text{and} \quad b_1 = -\hat{q}$$

where we have taken $B = C$, since flapping and in-plane moments of inertia of the blade are almost identical – typically, $C \approx 1.003B$.

When the pitching rate q is not constant, eqn 1.3 becomes ($e = 0$)

$$\frac{d^2\beta}{d\psi^2} + \frac{\gamma}{8}\frac{d\beta}{d\psi} + \beta = \frac{\gamma}{8}\hat{q}(\psi)\cos\psi - 2\hat{q}(\psi)\sin\psi + \frac{d\hat{q}}{d\psi}\cos\psi \tag{1.18}$$

According to the theory of differential equations there is a solution in the form

$$\beta = a_0(\psi) - a_1(\psi)\cos\psi - b_1(\psi)\sin\psi \tag{1.19}$$

where, as indicated, the flapping coefficients are no longer constants, as in the previous cases, but functions of time or azimuth angle.

The case of sinusoidally varying pitching velocity, which is important in stability investigations, has been analysed by Sissingh[2] and Zbrozek[3]. Taking $q = q_0 \sin\nu\psi$ and substituting eqn 1.19 into eqn 1.18 gives, after equating coefficients of $\sin\psi$ and $\cos\psi$,

$$\frac{\gamma}{8}a_1 + 2\frac{da_1}{d\psi} - \frac{\gamma}{8}\frac{db_1}{d\psi} - \frac{d^2b_1}{d\psi^2} = -2\hat{q}_0 \sin\nu\psi$$

$$\frac{\gamma}{8}\frac{da_1}{d\psi} + 2\frac{d^2a_1}{d\psi^2} + \frac{\gamma}{8}b_1 + 2\frac{db_1}{d\psi} = \hat{q}_0\nu\cos\nu\psi$$

The solutions for $a_1(\psi)$ and $b_1(\psi)$ are straightforward, but rather lengthy. Sissingh has shown that the tip path plane oscillates relative to the shaft, performing a beat motion out of phase with the shaft oscillation. Now, ν is the ratio of the pitching frequency to the rotational frequency of the shaft and in typical disturbed motion is usually much less than 0.1. On this basis Zbrozek has shown that, to good approximations, the lengthy expressions for a_1 and b_1 can be reduced to

$$a_1 \approx -16\hat{q}/\gamma + [(16/\gamma)^2 - 1]d\hat{q}/d\psi$$

$$b_1 \approx -\hat{q} + (24/\gamma)\,\mathrm{d}\hat{q}/\mathrm{d}\psi$$

Since a typical lateral or longitudinal stability oscillation is about 10 seconds, and the period of the rotor is about $\frac{1}{4}$ second (240 rev/min), ν is about 0.025. With $\hat{q} = \hat{q}_0 \sin \nu\psi$, the second terms of a_1 and b_1 are quite small and by neglecting them Zbrozek's expressions for a_1 and b_1 become the same as for the steady case. Thus, in disturbed motion, both a_1 and b_1 are proportional to q, and the rotor responds as if the instantaneous values were steady. This is the justification for the 'quasi-steady' treatment of rotor behaviour in which the rotor response is calculated as if the continuously changing motion were a sequence of steady conditions. This assumption greatly simplifies stability and control investigations. The 'quasi-static' behaviour of the rotor might also have been expected from its response as a second order system. The impressed motion considered above corresponds to forcing at a very low frequency ratio, and it is well known that the response is almost the same as if the instantaneous value of the forcing function were applied statically.

If the rolling case is considered, with constant angular velocity and $\varepsilon = 0$ as in the pitching case, it can be shown that the equivalent to eqn 1.16 is

$$\frac{\mathrm{d}^2\beta}{\mathrm{d}\psi^2} + \frac{\gamma}{8}\frac{\mathrm{d}\beta}{\mathrm{d}\psi} + \beta = \frac{\gamma}{8}\hat{p}\sin\psi + 2\hat{p}\cos\psi \qquad (1.16a)$$

in which $\hat{p} = p/\Omega$.

1.7 The cyclic and collective pitch control

The development of a satisfactory feathering mechanism was the last link in the creation of a successful helicopter and it enabled the rotor to be controlled without tilting the hub or shaft, as had been possible with the free-wheeling autogyro rotor. A brief description of the feathering mechanism is given below.

The principal feature of the feathering system is the swash plate mechanism, Fig. 1.13. This consists of two plates, of which the lower plate does not rotate with the shaft but can be tilted in any direction by the pilot's cyclic control. The upper plate rotates with the shaft but is constrained to remain parallel to the lower plate. It can be seen that if the swash plates are tilted the blade chord remains parallel to the swash plate and, as the blade rotates with the shaft, cyclic feathering takes place relative to

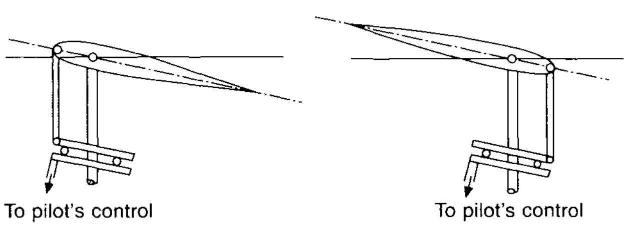

Fig. 1.13 Swash plate mechanism

the plane perpendicular to the shaft. The swash plate is, of course, a plane of no-feathering, and the axis through the centre of the hub and perpendicular to the swash plates is the no-feathering axis. Figure 1.5(b) shows a typical swash plate control mechanism.

Other feathering mechanisms have been employed such as that in Fig. 1.6(a), but the one described above is used a majority of helicopters.

Collective (constant) pitch is applied by the collective lever which effectively raises or lowers the swash plate without introducing further tilt; this alters the pitch angle of all the blades by the same amount.

1.8 Lagging motion

The lagging-motion equation, eqn 1.6, is

$$\ddot{\xi} + \Omega^2\varepsilon\xi - 2\Omega\beta\dot{\beta} = N/C$$

or

$$d^2\xi/d\psi^2 + \varepsilon\xi - 2\beta\, d\beta/d\psi = N/C\Omega^2 \tag{1.20}$$

where, as explained in section 1.4, the term $2\Omega\beta\dot{\beta}$ represents the Coriolis moment due to blade flapping.

In finding the free lagging motion, we assume the flapping motion to be absent and take N to be the aerodynamic (drag) moment of the blade about the lag hinge.

Let $d\Omega^2$ be the drag of the blade when it rotates at steady angular velocity Ω. The lagging motion increases the instantaneous angular velocity of the blade to $\Omega + \dot{\xi}$ and the drag can be assumed to be $d(\Omega + \dot{\xi})^2$. Since $\dot{\xi}$ is small compared with Ω, the drag is approximately $d\Omega^2 + 2d\Omega\dot{\xi}$. If R_D is the distance of the centre of drag of the blade from the hub, and assuming the lag hinge offset to be small,

$$N = -\,dR_D(\Omega^2 + 2\Omega\dot{\xi})$$

But $dR_D\Omega^3$ is the power, P say, required to drive one blade. Therefore

$$N = -(P/\Omega)(1 + 2\dot{\xi}/\Omega)$$

so that eqn 1.20 can be written

$$d^2\xi/d\psi^2 + (2P/C\Omega^3)d\xi/d\psi + \varepsilon\xi = -P/C\Omega^3 \tag{1.21}$$

Equation 1.21 is the equation of damped harmonic motion about a steady value $\xi = -P/C\Omega^3\varepsilon$. Typical values of $P/C\Omega^3$ and ε are 0.006 and 0.075 respectively, giving a steady value of ξ of about $4\frac{1}{2}$°. The frequency of oscillation is 0.27Ω and the damping is only about 2 per cent of critical. The much lower damping of the lagging mode is due to the fact that the blade motion in this case is governed by the changes of drag, and not of incidence. This low natural damping is usually augmented by hydraulic or elastomeric damping to avoid potential instability problems.

1.9 Lagging motion due to flapping

It will be assumed that the lag hinges are parallel to the rotor shaft so that ξ represents a change of blade angle in the plane of the hub, as in the previous section. The flapping motion must also be taken relative to this plane, and we will assume it takes the form $\beta = a_0 - a_1 \cos \psi$. In some later work we will have to distinguish flapping relative to the shaft from that relative to the no-feathering axis by writing $\beta_s = a_{0s} + a_{1s} \cos \psi$.

Regarding the Coriolis moment due to flapping as a forcing function, and ignoring the damping, we rewrite eqn 1.20 as

$$d^2\xi/d\psi^2 + \varepsilon\xi = 2\beta\, d\beta/d\psi + N/C\Omega^2 \tag{1.20a}$$

and we have to consider the meaning of the moment N in this case. Since the blade lift is perpendicular to the flow direction, the axis of the aerodynamic flapping moment must lie in the tip path plane, because this is the plane in which the blades move steadily. Thus there must be a component of the flapping moment about the lag hinge, and it is clear from Fig. 1.14 that this component is $-M_A a_1 \sin \psi$ and is equal to N.

But, we have seen that, for first harmonic flapping, and assuming zero flapping hinge offset, $M_A = B\Omega^2 a_0$, as explained in section 1.6.2. Therefore

$$N/C\Omega^2 = -a_0 a_1 \sin \psi$$

and, using the assumed form of $\beta = a_0 - a_1 \cos \psi$, then

$$2\beta\, d\beta/d\psi + N/C\Omega^2 = a_0 a_1 \sin \psi - a_1^2 \sin 2\psi$$

where, again, we have taken $B = C$. The solution to eqn 1.20a is

$$\xi = -[a_0 a_1/(1 - \varepsilon)] \sin \psi + [a_1^2/(4 - \varepsilon)] \sin 2\psi$$

The second term is generally smaller than the first and, since, ε is very small, to a fair approximation ξ can be written

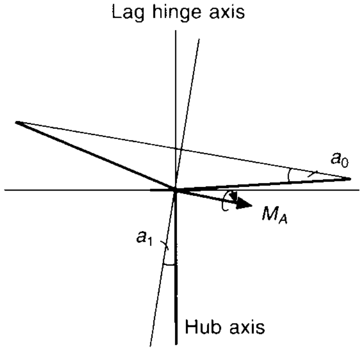

Fig. 1.14 Aerodynamic flapping moment component about lag hinge

$$\xi = -a_0 a_1 \sin \psi \tag{1.22}$$

Thus, the flapping motion forces a lagging motion which lags the flapping motion by 90°.

Equation 1.22 has a simple physical explanation. It can be seen from Fig. 1.15 that the blade movement about the lag hinge, i.e. in the hub plane, is simply steady motion of the blade in the tip path plane projected onto the hub plane. In other words, the ξ motion calculated above corresponds to uniform motion in the tilted rotor cone, and this is a result we should expect, for, since the flapping angle is constant relative to the tip path plane, there can be no Coriolis moments in this plane and the blade must rotate with constant angular velocity.

1.10 Feathering motion

For small pitch angles the blade feathering equation can be written

$$d^2\theta/d\psi^2 + \theta = L/A\Omega^2 \tag{1.23}$$

For free motion, $L = 0$, and the blade oscillates with shaft frequency. If θ is held constant, corresponding to collective pitch application, there will be a moment $A\Omega^2\theta$ trying to feather the blade into fine pitch. This moment is called the 'feathering moment' and must be resisted by the feathering mechanism. The fact that the natural

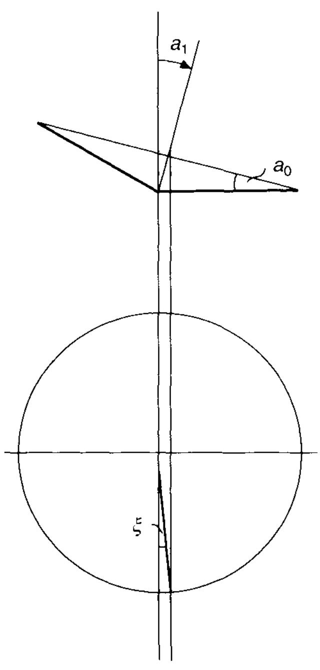

Fig. 1.15 Blade lagging motion due to flap

frequency of the feathering motion is exactly one cycle per revolution of the shaft – exactly as required – means that, except to overcome friction, no forces are necessary in the control links to maintain the motion.

The feathering moment $A\Omega^2\theta$ can be explained in terms of the centrifugal forces acting on the blade. In Fig. 1.16, AA′ is a chord of the blade. Consider elementary masses at the leading and trailing edges of the blade. The centrifugal forces acting on these masses are inclined outwards and, therefore, have components in opposite directions. But the centrifugal force directions both lie in planes perpendicular to the shaft so that when the blade is pitched the opposite directed components exert a couple tending to feather the blade into fine pitch. Integrating this moment in the chordwise and spanwise directions can be shown to lead to $A\Omega^2\theta$.

As with the flapping motion, the centrifugal moment acts like a spring giving a frequency exactly equal to that of the shaft, but, again like the flapping motion, if the feathering motion is viewed from a plane passing through the chord, the feathering motion vanishes and the centrifugal moment in this plane also vanishes, Fig. 1.17.

1.11 Rotor forces and moments

So far we have derived the equations of blade flapping, lagging, and feathering and have considered some simple cases of blade motion to illustrate some of its dynamic properties. We now have to consider the effect of this blade motion on the helicopter as a whole. We shall derive expressions for the forces and moments on the helicopter

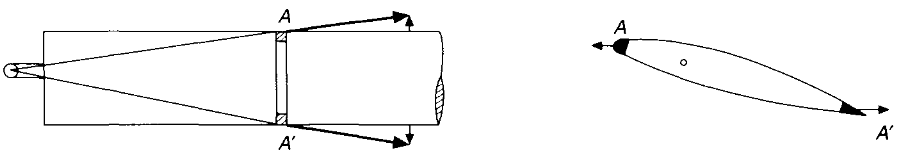

Fig. 1.16 Feathering moment

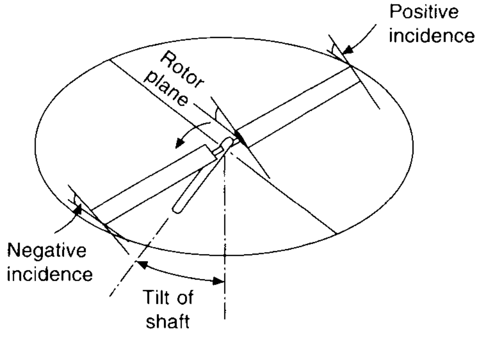

Fig. 1.17 Feathering in tip path plane due to rotor tilt

and consider requirements for trimmed flight. These requirements will appear as the control angles necessary to establish a given flight condition analogous to the static stability analysis of the fixed wing aircraft.

In order to be able to write down the equations of motion of the helicopter in steady and accelerated flight, it is necessary to calculate the forces exerted by the blade on the hub. To do this we shall have to relate the motion expressed in terms of axes fixed in the blade to axes fixed in the rotating hub and then to axes fixed in the helicopter.

As before, let, $\boldsymbol{i}, \boldsymbol{j}, \boldsymbol{k}$ be the set of unit axes fixed in the blade. Let $\boldsymbol{e}_1$, $\boldsymbol{e}_2$, $\boldsymbol{e}_3$ be a set of unit axes fixed in the rotating hub, Fig. 1.18.

When the blade is in its undeflected position, i.e. when there is no flapping or lagging, the blade axes coincide with the hub axes. Now, suppose the blade flaps through angle β about $\boldsymbol{e}_2$, bringing the blade axes into a position whose unit vectors are $\boldsymbol{i}_1, \boldsymbol{j}_1, \boldsymbol{k}_1$. The relationships between $\boldsymbol{e}_1$, $\boldsymbol{e}_2$, $\boldsymbol{e}_3$ and $\boldsymbol{i}_1, \boldsymbol{j}_1, \boldsymbol{k}_1$ are related through a rotation matrix transformation as

$$\begin{bmatrix} \boldsymbol{i}_1 \\ \boldsymbol{j}_1 \\ \boldsymbol{k}_1 \end{bmatrix} = \begin{bmatrix} \cos\beta & 0 & \sin\beta \\ 0 & 1 & 0 \\ -\sin\beta & 0 & \cos\beta \end{bmatrix} \begin{bmatrix} \boldsymbol{e}_1 \\ \boldsymbol{e}_2 \\ \boldsymbol{e}_3 \end{bmatrix} \tag{1.24}$$

The blade now rotates about the lag axis through angle ξ, bringing the unit vectors of the blade into their final positions $\boldsymbol{i}, \boldsymbol{j}, \boldsymbol{k}$. The relationships between $\boldsymbol{i}, \boldsymbol{j}, \boldsymbol{k}$ and $\boldsymbol{i}_1$, $\boldsymbol{j}_1$, $\boldsymbol{k}_1$, are, in matrix form

$$\begin{bmatrix} \boldsymbol{i} \\ \boldsymbol{j} \\ \boldsymbol{k} \end{bmatrix} = \begin{bmatrix} \cos\xi & \sin\xi & 0 \\ -\sin\xi & \cos\xi & 0 \\ 0 & 0 & 1 \end{bmatrix} \begin{bmatrix} \boldsymbol{i}_1 \\ \boldsymbol{j}_1 \\ \boldsymbol{k}_1 \end{bmatrix} \tag{1.25}$$

The relationships between $\boldsymbol{e}_1$, $\boldsymbol{e}_2$, $\boldsymbol{e}_3$ and $\boldsymbol{i}, \boldsymbol{j}, \boldsymbol{k}$, are on multiplying the transformation matrices in eqns 1.24 and 1.25 together

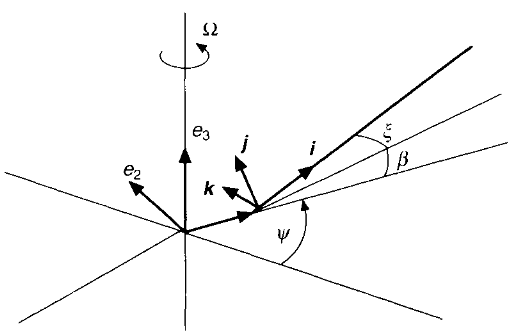

Fig. 1.18 Deflected rotating blade

$$\begin{bmatrix} \boldsymbol{i} \\ \boldsymbol{j} \\ \boldsymbol{k} \end{bmatrix} = \begin{bmatrix} \cos\xi\cos\beta & \sin\xi & \cos\xi\sin\beta \\ -\sin\xi\cos\beta & \cos\xi & -\sin\xi\sin\beta \\ -\sin\beta & 0 & \cos\beta \end{bmatrix} \begin{bmatrix} \boldsymbol{e}_1 \\ \boldsymbol{e}_2 \\ \boldsymbol{e}_3 \end{bmatrix} \tag{1.26}$$

The above relationships enable us to express quantities measured in one set of axes in terms of another set, and we shall need them for calculating the forces and moments on the helicopter.

Let the distance of the centre of gravity of the blade measured from the hinge be r_g. In terms of axes fixed in the blade the position vector of the c.g. is $\boldsymbol{r}_g = r_g\boldsymbol{i}$, and in terms of hub axes the position vector is

$$\boldsymbol{r}_g + eR\boldsymbol{e}_1 = r_g(\cos\beta\cos\xi\boldsymbol{e}_1 + \sin\xi\boldsymbol{e}_2 + \sin\beta\cos\xi\boldsymbol{e}_3) + eR\boldsymbol{e}_1$$

Expressing the absolute acceleration $\boldsymbol{a}_g$ of the c.g. as $\boldsymbol{a}_g = a_1\boldsymbol{e}_1 + a_2\boldsymbol{e}_2 + a_3\boldsymbol{e}_3$, the components, by applying the standard equations of the kinematics of a rigid body, are found to be

$$a_1 = r_g \frac{d^2}{dt^2}(\cos\beta\cos\xi) - 2r_g\Omega\frac{d}{dt}(\sin\xi) - \Omega^2(r_g\cos\beta\cos\xi + eR) \tag{1.27}$$

$$a_2 = r_g \frac{d^2}{dt^2}(\sin\xi) + 2r_g\Omega\frac{d}{dt}(\cos\beta\cos\xi) - \Omega^2 r_g\sin\xi \tag{1.28}$$

$$a_3 = r_g \frac{d^2}{dt^2}(\sin\beta\cos\xi) \tag{1.29}$$

Now, let the aerodynamic force on the blade be $\boldsymbol{F}$ and let $\boldsymbol{R}$ be the force exerted by the hinge on the blade. If M_b is the blade mass, the equation of motion is

$$\boldsymbol{F} + \boldsymbol{R} = M_b\boldsymbol{a}_g \tag{1.30}$$

If $\boldsymbol{F} = F_1\boldsymbol{e}_1 + F_2\boldsymbol{e}_2 + F_3\boldsymbol{e}_3$ and $\boldsymbol{R} = R_1\boldsymbol{e}_1 + R_2\boldsymbol{e}_2 + R_3\boldsymbol{e}_3$,

$$\left.\begin{aligned} R_1 &= M_b a_1 - F_1 \\ R_2 &= M_b a_2 - F_2 \\ R_3 &= M_b a_3 - F_3 \end{aligned}\right\} \tag{1.31}$$

We now wish to resolve these rotating force components along axes fixed in the helicopter. In order to comply with the usual stability axes, we take a set of unit axes $\boldsymbol{x}$, $\boldsymbol{y}$, z, with the z axis pointing downwards along the negative direction of $\boldsymbol{e}_3$, Fig. 1.19.

If X, Y, Z are the hub force components along the fixed axes, then, remembering that the force the blade exerts on the hub is $-\boldsymbol{R}$,

$$X = R_1\cos\psi - R_2\sin\psi$$

$$Y = -R_1\sin\psi - R_2\cos\psi$$

$$Z = R_3$$

These forces are time dependent, not only because of the sin ψ and cos ψ terms,

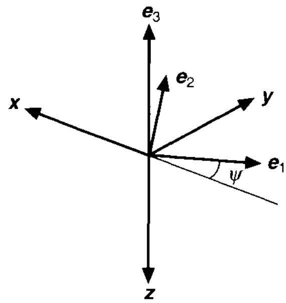

Fig. 1.19 Blade and helicopter axes

but because the aerodynamic force will also be a function of the azimuth angle. For performance and stability calculations we are interested in the time-averaged values. Consider the average value of X taken over a complete revolution. We have

$$\int_0^\tau X\,\mathrm{d}t = M_b \int_0^\tau a_1 \cos\psi\,\mathrm{d}t - \int_0^\tau F_1 \cos\psi\,\mathrm{d}t$$

$$-M_b \int_0^\tau a_2 \sin\psi\,\mathrm{d}t + \int_0^\tau F_2 \sin\psi\,\mathrm{d}t$$

where τ is a complete period.

Now, from eqn 1.27, the first term of a_1 is $r_g\,\mathrm{d}^2(\cos\beta\cos\xi)/\mathrm{d}t^2$. Integrating twice by parts,

$$\int_0^\tau \frac{\mathrm{d}^2}{\mathrm{d}t^2}(\cos\beta\cos\xi)\cos\psi\,\mathrm{d}t = \left[\frac{\mathrm{d}}{\mathrm{d}t}(\cos\beta\cos\xi)\cos\psi\right]_0^\tau$$

$$+\Omega\left[\cos\beta\cos\xi\sin\psi\right]_0^\tau - \Omega\int_0^\tau \cos\beta\cos\xi\cos\psi\,\mathrm{d}t$$

If the other terms involving a_1 and a_2 are integrated in a similar way, we find that, if the motion is periodic, i.e. if the flight condition is steady, all the terms in the brackets vanish at the limits and all the remaining integrals cancel identically.

In other words, the mean values of all the inertia forces are zero and the only forces which remain are the aerodynamic forces. The vanishing of the inertia forces in steady unaccelerated flight might have been expected on physical grounds, but it is a common mistake to believe that this is not necessarily the case; the reason for this is that small angle approximations for the flapping and lagging angles are often made when resolving the inertia forces, and considerable residuals may remain, particularly as the centrifugal force is extremely large[4].

The mean forces are therefore

$$(1/\tau)\int_0^\tau X\,\mathrm{d}t = \bar{X} = -(1/\tau)\int_0^\tau F_1\cos\psi\,\mathrm{d}t + (1/\tau)\int_0^\tau F_2\sin\psi\,\mathrm{d}t \qquad (1.32)$$

$$(1/\tau)\int_0^\tau Y\,\mathrm{d}t = \overline{Y} = (1/\tau)\int_0^\tau F_1 \sin\psi\,\mathrm{d}t + (1/\tau)\int_0^\tau F_2 \cos\psi\,\mathrm{d}t \qquad (1.33)$$

$$(1/\tau)\int_0^\tau Z\,\mathrm{d}t = \overline{Z} = (1/\tau)\int_0^\tau F_3\,\mathrm{d}t \qquad (1.34)$$

The force components $\overline{X}$ and $\overline{Y}$ in the plane of the hub give rise to pitching and rolling moments about the helicopter's centre of gravity. Further, the force at the offset hinge, in the direction of the shaft, also exerts pitching and rolling moments. This force has the same magnitude as Z, so that, if hR is the height of the hub above the c.g. and eR is the distance of the hinge from the shaft axis, the average rolling moment per blade on the helicopter is

$$\begin{aligned} L &= \overline{Y}hR + \frac{eR}{\tau}\int_0^\tau Z\sin\psi\,\mathrm{d}t \\ &= \overline{Y}hR + \frac{M_\mathrm{b}ex_\mathrm{g}R^2}{\tau}\int_0^\tau \frac{\mathrm{d}^2}{\mathrm{d}t^2}(\sin\beta\cos\xi)\sin\psi\,\mathrm{d}t - \frac{eR}{\tau}\int_0^\tau F_3\sin\psi\,\mathrm{d}t \\ &= \overline{Y}hR - \frac{M_\mathrm{b}ex_\mathrm{g}\Omega^2R^2}{2\pi}\int_0^{2\pi}\sin\beta\cos\xi\sin\psi\,\mathrm{d}\psi - \frac{eR}{2\pi}\int_0^{2\pi} F_3\sin\psi\,\mathrm{d}\psi \qquad (1.35)\end{aligned}$$

in which $x_\mathrm{g}R = r_\mathrm{g}$.

Similarly, the pitching moment M per blade is

$$M = -\overline{X}hR - \frac{M_\mathrm{b}ex_\mathrm{g}\Omega^2R^2}{2\pi}\int_0^{2\pi}\sin\beta\cos\xi\cos\psi\,\mathrm{d}\psi - \frac{eR}{2\pi}\int_0^{2\pi} F_3\cos\psi\,\mathrm{d}\psi \qquad (1.36)$$

The first integrals in L and M are the inertia couples which arise when the plane of a rotor with offset hinges is tilted relative to the shaft. If the flapping motion relative to the shaft is $\beta_\mathrm{s} = a_0 - a_{1\mathrm{s}}\cos\psi - b_{1\mathrm{s}}\sin\psi$, then, for small β and ξ, these integrals are $\frac{1}{2}M_\mathrm{b}ex_\mathrm{g}\Omega^2R^2b_{1\mathrm{s}}$ and $\frac{1}{2}M_\mathrm{b}ex_\mathrm{g}\Omega^2R^2a_{1\mathrm{s}}$ respectively.

The second integrals in L and M are found to be very much smaller and can be neglected, so that to a good approximation

$$\begin{aligned} L &= \overline{Y}hR + \tfrac{1}{2}M_\mathrm{b}ex_\mathrm{g}\Omega^2R^2b_{1\mathrm{s}} \\ &= \overline{Y}hR + \tfrac{1}{2}SeRb_{1\mathrm{s}} \qquad (1.37)\end{aligned}$$

and

$$M = -\overline{X}hR + \tfrac{1}{2}SeRa_{1\mathrm{s}} \qquad (1.38)$$

where $S = M_\mathrm{b}x_\mathrm{g}\Omega^2R$ is the centrifugal force of the blade for zero offset, and approximately so for small offset.

For the small hinge offsets that are usual, the second terms of eqns 1.37 and 1.38 can be interpreted, in the case of two opposing blades, as the couple due to the displaced centrifugal force vectors, and these are parallel to the tip path plane which is the plane of steady rotation, Fig. 1.20. For small offsets, the inclination of the tip path plane is approximately equal to the flapping angle.

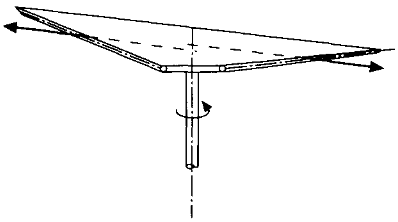

Fig. 1.20 Centrifugal force couple on tilted rotor with offset hinges

1.12 Rotor forces and choice of axes

In the previous section, the rotor force components were expressed in terms of a set of axes fixed in the helicopter. As explained there, such a formulation is necessary to study the forces and moments on the whole helicopter. However, it is more usual, and natural, when considering the rotor as a lifting device, to regard it as producing a thrust, defined along some convenient direction, together with small components of force in the other two perpendicular directions. For this purpose, three axes systems are in common use, as follows. The question as to which axis is the most useful depends upon the problem being considered, and will become apparent in the applications dealt with later, although some indications are given below.

1.12.1 The no-feathering or control axis

As explained in section 1.6.2, this is the axis normal to the plane of the swash plate. By definition, no cyclic feathering occurs relative to this axis, the blade pitch being the constant value supplied by the collective pitch application. Since the pitch angle is constant, the only other blade motion contribution to the local blade incidence is that due to the flapping. The no-feathering axis is often used to express the blade flapping, especially when blade aerodynamic forces are being established, since constant blade pitch at a section eases the mathematical development. The rotor aerodynamics and dynamics established in Chapter 3 are expressed using this axis system.

1.12.2 The tip path plane or disc axis

The tip path plane axis is the axis perpendicular to the plane through the blade tips and, for zero offset flapping hinges, it is therefore the axis of no flapping. The definition applies only to first harmonic motion since, when there are higher harmonics, the blades no longer trace out a plane. Of the higher harmonics, only the odd values affect the tilt of the disc, and these are usually extremely small compared with the first harmonics, as explained in section 1.6.2. Now, although there is no first harmonic flapping relative to the tip path plane, there will be cyclic feathering and the amount of feathering is exactly equal to the flapping relative to the no-feathering axis. Thus, in this case, the blade incidence will be determined from the collective pitch and the apparent feathering motion in the tip path plane.

When the flapping hinges are offset, the tip path plane axis is no longer the axis of no flapping, as can be easily seen from a diagram like Fig. 1.20 with exaggerated hinge offset. Strictly speaking, both feathering and flapping occur relative to the tip path plane but, provided the offset is small, as it usually is, the error in assuming that there is no flapping is negligible.

1.12.3 The shaft or hub plane axis

This axis is usually less convenient for calculating the rotor forces, as the blade incidence must be expressed in terms of both feathering and flapping. It is, nevertheless, a useful axis for dealing with hingeless rotors, since blade flapping relative to the hub is of prime importance. Indeed, the blade mechanics developed so far in the current chapter have been with reference to the shaft axis.

1.13 The rotor disc

In all the three cases discussed above, it is usual to call the force component along the axis, whichever of the above it is, the thrust T. The component perpendicular to this axis and pointing rearward is called the H force, and the third component, pointing sideways to starboard, is the Y force. Usually the Y force is very small and attention is mainly focused on the thrust and the H force, i.e. the longitudinal force components. Calculations and measurements show that the resultant rotor force is almost perpendicular to the tip path plane, usually pointing backwards slightly. It is for this reason that the tip path plane axis is useful since the resultant force is almost exactly equal to the thrust; the H force can be regarded as a kind of rotor drag.

Let us denote the thrust and the H force relative to the no-feathering axis by T and H respectively, and use the subscript D to denote the tip path plane (disc) axis and S to denote the shaft axis. Now the flapping and feathering angles are usually small – larger than 10° would be regarded as extreme values – so that, referring to Fig. 1.21, the approximate relations between the thrust and forces referred to the different axes are

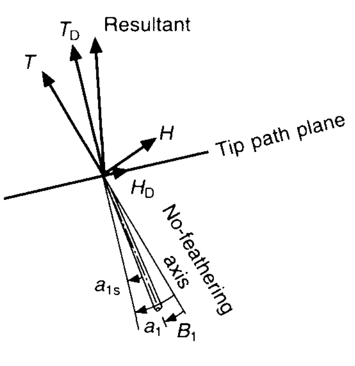

Fig. 1.21 Thrust and H-force vectors

$$T \approx T_D \approx T_s \tag{1.39}$$

$$H \approx H_D + T_D a_1 \approx H_s + T_s B_1 \tag{1.40}$$

where B_1 is the amplitude of the longitudinal cyclic pitch.

1.14 Longitudinal trim equations

The foregoing analysis in this chapter has provided the main features of rotor behaviour, and demonstrated the dependence of rotor forces on the various different parameters involved. By extending the analysis to include the helicopter fuselage whilst maintaining the simplified rotor model, it is possible to derive the equations of equilibrium in steady, uniform, trimmed flight. From this, the attitude of the fuselage may be determined. These exercises are done for longitudinal flight in this and the following section, and lateral control to trim is studied in the final section 1.16.

Referring to Fig. 1.22, and resolving forces in the vertical direction,

$$W + D \sin \tau_c = T \cos (\theta - B_1) - H \sin (\theta - B_1) \tag{1.41}$$

and, resolving horizontally,

$$D \cos \tau_c = - T \sin (\theta - B_1) - H \cos (\theta - B_1) \tag{1.42}$$

where θ is the angle between the vertical and shaft, positive nose up, and τ_c is the angle of climb. Since θ and B_1 are small angles, eqns 1.41 and 1.42 can be written approximately as

$$W + D \sin \tau_c = T \tag{1.43}$$

$$H + D \cos \tau_c = T(B_1 - \theta) \tag{1.44}$$

Since $D \sin \tau_c$ is very much smaller than W, then $T \approx W$.

The origin of moments O is defined as the point on the shaft met by the perpendicular from the c.g. If hR is the height of the hub above this point, and lR the distance of the

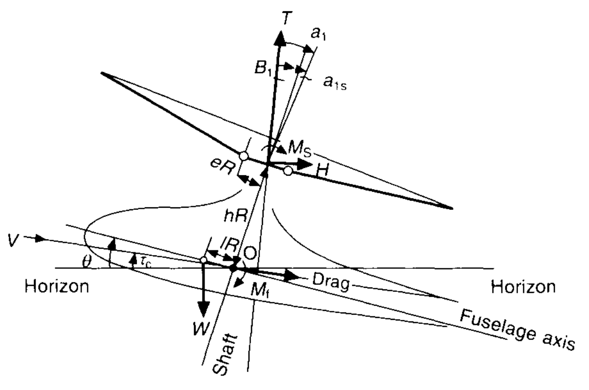

Fig. 1.22 Forces and moments in longitudinal plane

c.g. forward of this point, taking moments about O and making the small angle assumption gives

$$-WlR - ThRB_1 + HhR + M_f - M_s(B_1 - a_1) = 0 \tag{1.45}$$

where M_f is the fuselage pitching moment and $M_s = f_b SeR$ is the centrifugal moment per unit tilt of all the blades (eqn 1.38), and f_b is a factor depending on the number of blades.

Solving eqn 1.45 for B_1 gives

$$B_1 = (M_f - WlR + HhR + M_s a_1)/(ThR + M_s) \tag{1.46}$$

Equation 1.46 gives the longitudinal cyclic pitch required for trim. For very small or zero offset, we can put $M_s = 0$ and, since $T \approx W$, we have

$$B_1 = M_f/WhR - l/h + H/W \tag{1.47}$$

and, if the fuselage pitching moment $M_f = 0$,

$$B_1 = -l/h + H/W \tag{1.48}$$

The denominator of the right-hand side of eqn 1.46 represents the control moment for unit displacement of the rotor disc relative to the hub axis. The term ThR is the moment due to the tilt of the thrust vector, which is the only control moment acting if the hinges are centrally located ($e = 0$) or the rotor is of the see-saw type. M_s is the centrifugal couple due to the flapping hinge offset, section 1.11. We shall see in Chapter 4 that for a typical offset distance, $e = 0.04$ say, the total moment is more than doubled by the offset hinge contribution.

The importance of the offset hinge moment is that it not only augments the control power but is also independent of the thrust and can be designed to provide adequate control power in those flight conditions where the thrust is temporarily reduced, e.g. the 'push-over' manoeuvre or the transition from powered flight to autorotation.

Equation 1.48 has a simple physical interpretation: the longitudinal cyclic pitch B_1 must be such as to make the resultant rotor force pass through the helicopter's centre of gravity, Fig. 1.23; the figure shows that $B_1 + l/h = \tan^{-1}(H/T) \approx H/W$, which is eqn 1.48.

If M_s and M_f are not zero, the resultant force vector no longer passes through the c.g. but must exert a moment about it in order to balance the M_s and M_f moments.

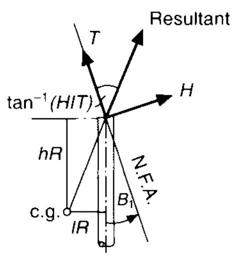

Fig. 1.23 Resultant rotor force vector

Expressed in terms of the tip path plane, eqn 1.47 becomes

$$B_1 = a_1 + H_D/W - l/h + M_f/WhR \tag{1.49}$$

Now H_D, the force component in the plane of the rotor disc, is usually quite small, so that for given values of l/h and M_f, the cyclic pitch to trim is roughly that required to eliminate the backward flapping of the rotor. This is a convenient way of interpreting the cyclic pitch to trim and shows the advantage of using the tip path plane as a reference plane in this case. With $M_f = 0$, Fig. 1.23 can be redrawn as Fig. 1.24.

1.15 The attitude of the helicopter

Since $T \approx W$, eqn 1.44 can be written

$$(D/W) \cos \tau_c + H/W = B_1 - \theta \tag{1.50}$$

Eliminating B_1 by means of eqn 1.46 gives

$$\theta = -\frac{D \cos \tau_c}{W} - \frac{H}{W} + \frac{M_f - WlR + HhR + M_s a_1}{WhR + M_s} \tag{1.51}$$

If M_s is negligible,

$$\theta = -(D/W) \cos \tau_c - l/h + M_f/WhR$$

Thus, for a given c.g. position and supposing M_f to be constant, the helicopter fuselage attitude is directly proportional to the drag and, hence, the square of the speed. Another important conclusion is that, unlike a fixed wing aircraft, the attitude depends very little on the angle of climb for, since the angle of climb is contained only in $\cos \tau_c$ even quite steep climbs have little effect on $(D/W) \cos \tau_c$ and therefore on θ.

1.16 Lateral control to trim

Referring to Fig. 1.25, resolving horizontally, with $T \approx W$ and ignoring the sideways pointing Y force,

$$W(A_1 + b_1 + \phi) + T_t = 0 \tag{1.52}$$

where T_t is the tailrotor thrust.

Taking moments about O, and for small angles of bank,

$$WfR + WhR(A_1 + b_1) + M_s(A_1 + b_1) + T_t h_t R = 0 \tag{1.53}$$

where fR is the lateral displacement of the c.g. and $h_t R$ is the tailrotor height.

Solving eqn 1.53 for A_1 gives

$$A_1 = -b_1 - \frac{WfR + T_t h_t R}{WhR + M_s} \tag{1.54}$$

which is the lateral cyclic pitch to trim.

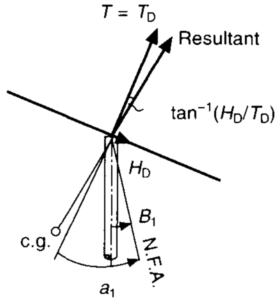

Fig. 1.24 Rotor force components in tip path (disc) plane

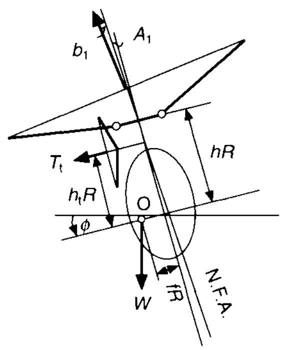

Fig. 1.25 Forces and moments in lateral plane

Eliminating A_1 from eqn 1.54 gives the trimmed bank attitude:

$$\phi = -\frac{T_t}{W} + \frac{WfR + T_t h_t R}{WhR + M_s} \tag{1.55}$$

If $M_s = 0$ (no offset hinge) and $h_t = h$, which is usually approximately true, then

$$\phi \approx f/h$$

which means that the c.g. lies vertically below the rotor, for the rotor thrust vector

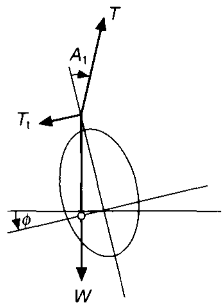

Fig. 1.26 Helicopter lateral attitude

must be tilted relative to the vertical to balance the tailrotor side force and tilted away from the c.g. to balance the tailrotor moment, Fig. 1.26.

References

1. Stewart, W., 'Higher harmonics of flapping on the helicopter rotor', *Aeronautical Research Council CP 121*, 1952.
2. Sissingh, G. J., 'The frequency response of the ordinary rotor blade, the Hiller servo-blade and the Young-Bell stabilizer', *Aeronautical Research Council R&M 2860*, 1950.
3. Zbrozek, J. K., 'The simple harmonic motion of a helicopter rotor with hinged blades', *Aeronautical Research Council R&M 2813*, 1949.
4. Correspondence in *Aircraft Engineering*, September and November 1955.